Synthesis and optical properties of LiCaY(MoO$_4$)$_3$:Eu^{3+} red phosphor with negligible concentration quenching for highly efficient white LED and plant growth applications

Priyansha Sharma[a], Jaya Prakash Madda[a] and Sivakumar Vaidyanathan[b*]

[a] Department of Chemistry, National Institute of Technology Rourkela - 769 008, Odisha, India.

[b] Department of Chemistry, Indian Institute of Technology Hyderabad, Sangareddy, Kandi, Telangana 502285, India.

---

[*] To whom correspondence should be addressed. Email: vsiva@chy.iith.ac.in (Sivakumar Vaidyanathan).

Characterization

The phase formation and purity of the phosphors were analyzed using powder X-ray diffractometer (RIGAKU, JAPAN & ULTIMA -IV) which utilizes Cu-Kα1 radiation for generation of X-rays. The SEM images were taken by JEOL JSM 6480LV scanning electron microscope. The FTIR was carried out in the range of 400 - 4000 cm^{-1} by Shimadzu, IR Prestige-21, an Automatic infrared microscope. The PL (excitation and emission) spectra and lifetime were monitored by using an Edinburgh Spectrofluorometer FS-5 instrument with attached SC-10 and SC-30 integrating sphere modules. A pulsed xenon lamp was used as the excitation source, and the signals were detected with a photomultiplier. Time-resolved PL and Temperature-dependent PL spectra were measured by using the spectrometer (HORIBA) equipped with a temperature controller. The Commission International de'Eclairage (CIE) color coordinates were calculated from CIE 1931 software. The CRI and color purity were calculated by color calculator software. All the measurements have been carried out at room temperature (RT).
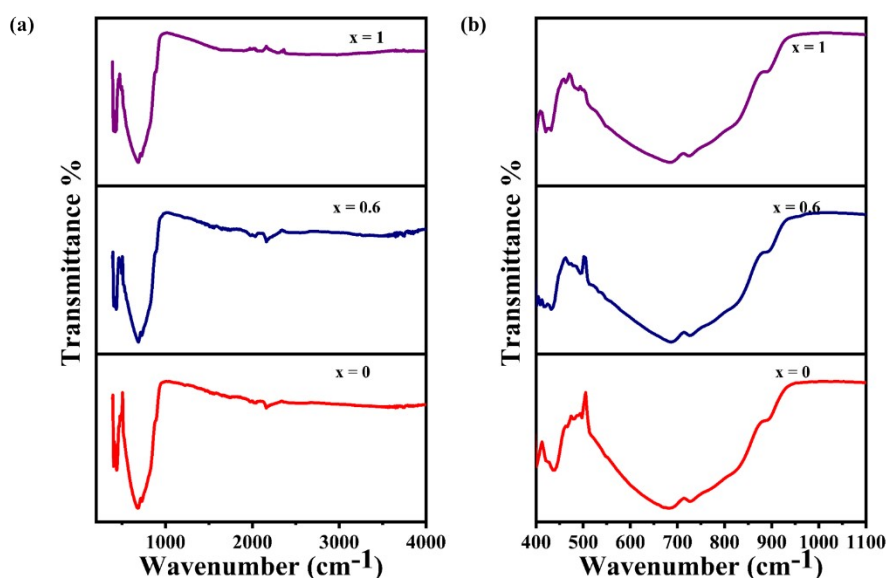

Figure S1: a) The FT-IR spectrum of LiCaYEu(MoO$_4$)$_3$ from (x = 0, 0.6, and 1) and b) Enlarged FT-IR spectra of LiCaYEu(MoO$_4$)$_3$ from (400-1100) cm^{-1}
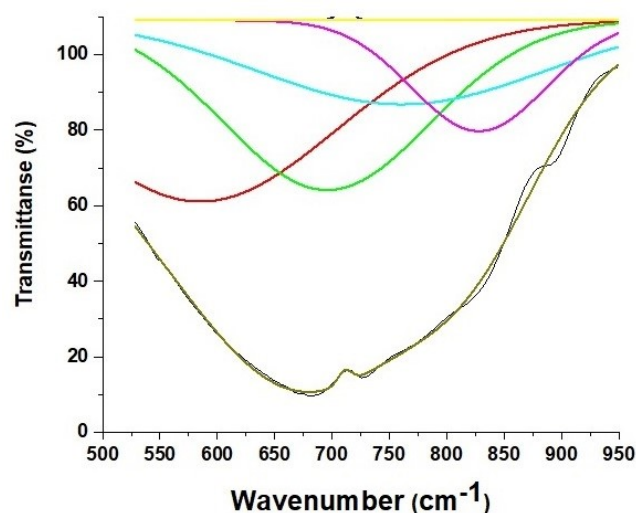
Figure S2: The FT-IR spectrum peak deconvolution for x = 0.

Table ST1: Deconvolution peak data for x = 0.

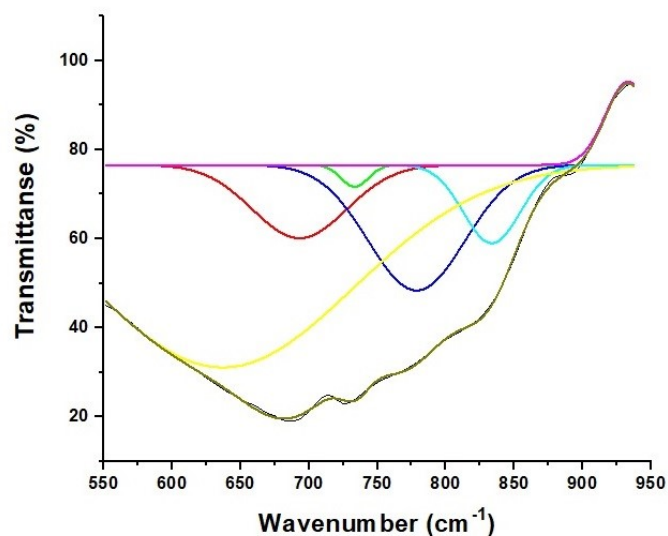| Model	Gaussian					
Equation	$y = y0 + A/(w*sqrt(pi/(4*ln(2)))) * exp(-4*ln(2)*(x-xc)^2/w^2)$					
Plot	Peak1(B)	Peak2(B)	Peak3(B)	Peak4(B)	Peak5(B)	Peak6(B)
y0	109.09446 ± 3757.82364	109.09446 ± 3757.82364	109.09446 ± 3757.82364	109.09446 ± 3757.82364	109.09446 ± 3757.82364	109.09446 ± 3757.82364
xc	585.05514 ± 264045.6067	695.83663 ± 28765.54281	711.0506 ± 2.35764	760.32304 ± 1782008.76328	827.90097 ± 58.36272	947.2121 ± 0
A	-14251.52611 ± 7.0464E7	-10106.71847 ± 6.23666E7	56.55687 ± 30.06084	-6959.29072 ± 1.36694E8	-4322.79302 ± 847025.42382	-4070719.24535 ± 0
w	278.90591 ± 52794.58278	211.1359 ± 114665.47757	14.82669 ± 6.59723	293.49839 ± 1077020.8938	138.34812 ± 2436.06347	0.00626 ± 0
Reduced Chi-Sqr	2.39706					
R-Square (COD)	0.99691					
Adj. R-Square	0.9963					

Figure S3: The FT-IR spectrum peak deconvolution for x = 0.6.

Table ST2: Deconvolution peak data for x = 0.6.

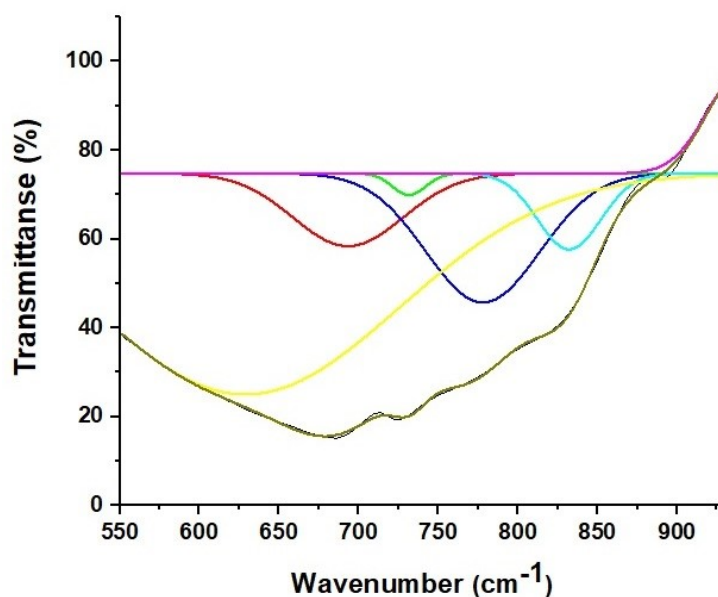| Model	Gaussian					
Equation	y = y0 + A/(w*sqrt(pi/(4*ln(2)))) * exp(-4*ln(2)*(x-xc)^2/w^2)					
Plot	Peak1(B)	Peak2(B)	Peak3(B)	Peak4(B)	Peak5(B)	Peak6(B)
y0	76.56623 ± 4.29762	76.56623 ± 4.29762	76.56623 ± 4.29762	76.56623 ± 4.29762	76.56623 ± 4.29762	76.56623 ± 4.29762
xc	693.1733 ± 10.89213	733.51695 ± 1.12013	778.75403 ± 3.10729	833.66886 ± 2.20902	933.21055 ± 1.18034	636.93074 ± 30.1082
A	-1423.19258 ± 1604.02166	-123.82694 ± 54.09814	-2492.6355 ± 1215.74239	-915.14118 ± 540.47107	774.90708 ± 185.27036	-10934.51476 ± 5301.50176
w	81.31392 ± 22.45041	23.76644 ± 4.40994	83.05262 ± 21.69228	48.90102 ± 6.74645	38.96323 ± 3.7766	225.80744 ± 64.20017
Reduced Chi-Sqr	0.28823					
R-Square (COD)	0.9995					
Adj. R-Square	0.99938					

4

Figure S4: The FT-IR spectrum peak deconvolution for x = 1.

Table ST3: Deconvolution peak data for x = 1.

Model	Gaussian					
Equation	y = y0 + A/(w*sqrt(pi/(4*ln(2)))) * exp(-4*ln(2)*(x-xc)^2/w^2)					
Plot	Peak1(B)	Peak2(B)	Peak3(B)	Peak4(B)	Peak5(B)	Peak6(B)
y0	74.79999 ± 4.72014	74.79999 ± 4.72014	74.79999 ± 4.72014	74.79999 ± 4.72014	74.79999 ± 4.72014	74.79999 ± 4.72014
xc	693.38467 ± 12.3521	731.68474 ± 1.46231	778.0182 ± 2.75968	832.22172 ± 2.13534	940.1967 ± 1.16961	628.9101 ± 27.26028
A	-1420.64913 ± 1746.27985	-127.56763 ± 67.99594	-2607.4187 ± 1315.14069	-854.31157 ± 549.71475	1236.39097 ± 302.07049	-12086.22212 ± 5622.38
w	81.43591 ± 25.54266	24.69568 ± 5.51281	84.24147 ± 26.30759	46.92653 ± 7.138	51.65742 ± 4.75141	227.95641 ± 65.70672
Reduced Chi-Sqr	0.40379					
R-Square (COD)	0.99946					
Adj. R-Square	0.99935					

Table ST4: Peak positions in all the above spectra for x = 0, 0.6 and 1.

	Peak maximum (wavenumber (cm⁻¹)			
	Peak-1	Peak-2	Peak-3	Peak-4
X = 0	695	711	827	947
X = 0.6	693	733	833	933
X = 1	693	731	832	940

Table. ST5 Electric dipole, magnetic dipole, and Asymmetry ratio of LCYM: Eu^{3+} phosphor calculated at ED transition.

Eu^{3+} Concentration	Electric dipole (616nm) $^5D_0/^7F_2$	Magnetic dipole (592 nm) $^5D_0/^7F_1$	ED/MD(AR)
0.2	23916040	1481897.63	16.14
0.4	44698624	2824559.2	15.82
0.6	52117052	3145710.5	16.56
0.8	74948728	4441308	16.87
1.0	65623348	3609866.5	18.17

Table. ST6 CIE coordinates, Color purity and Asymmetry ratio of LCYM: Eu^{3+} phosphor calculated at ED transition.

Eu^{3+} Concentration	CIE coordinates (x, y)	Colour purity	Asymmetry ratio
0.2	0.6624, 0.3369	95.4%	16.13
0.4	0.6663, 0.3331	96.4%	15.82
0.6	0.6680, 0.3316	96.8%	16.56
0.8	0.6692, 0.3304	97.1%	16.87
1.0	0.6699, 0.3297	97.3%	18.17

Table. ST7 CIE coordinates and Color purity of LCYM: Eu^{3+} phosphor calculated at 299 nm.

Eu^{3+} Concentration	CIE coordinates (x, y)	Colour purity
0.2	0.6645, 0.3349	95.9%
0.4	0.6655, 0.3339	96.1%
0.6	0.6684, 0.3311	96.9%
0.8	0.6690, 0.3305	97.10%
1.0	0.6694,0.3302	97.20%

Table. ST8 CIE coordinates and Color purity of LCYM: Eu^{3+} phosphor calculated at 465 nm.

Eu^{3+} Concentration	CIE coordinates (x,y)	Colour purity
0.2	0.6602,0.3388	94.84%
0.4	0.6637,0.3353	95.73%
0.6	0.6666,0.3327	96.48%
0.8	0.6676,0.3318	96.73%
1.0	0.6685,0.3309	96.97%

Table ST9 : Judd – Ofelt Parameters of LiCaY(MoO₄)₃:Eu³⁺ phosphor (300 nm)

Table ST9 : Judd – Ofelt Parameters of $LiCaY(MoO_4)_3:Eu^{3+}$ phosphor (300 nm)

Concentration of Eu^{3+}	Judd - Oflet Parameter		A_{0-1} in S^{-1}	A_{0-2} in S^{-1}	A_{0-4} in S^{-1}
	Ω_2 (10^{-19} cm²)	Ω_4 (10^{-20} cm²)			
0.4	1.0312	4.224	50	841.45858	166.7669
0.6	1.2146	4.306	50	995.45154	170.0455
0.8	1.1531	4.559	50	945.05709	180.2003
1.0	1.188	4.716	50	970.09486	185.8942